Conference Paper, Published Version

Feng, Jiawei; Jodeau, Magali

Three-dimensional numerical modeling of sediment transport with TELEMAC-3D: validation of test cases

Three-dimensional numerical modeling of sediment transport with TELEMAC-3D: validation of test cases

Jiawei Feng
Ecole Centrale de Nantes, France
jiawei.ecn@gmail.com

Magali Jodeau
EDF R&D LNHE, France
magali.jodeau@edf.fr

***Abstract*—The aim of this work is to validate specifically the proper calculation of TELEMAC-3D in numerical modeling of sediment transport. Generally, all the validation tests can be divided into two categories: (1) simulations with an analytical solution, existing exclusively in some special conditions (2) simulations deriving from physical experiments and in situ measurements with reliable initial, boundary and final conditions. Several validated cases are included in this paper and they will be included in the 8.0 release of TELEMAC, the first two belonging to the first category while the third belonging to the second. The first case is a simulation of a perfectly still settling basin containing water with an initial uniform sediment concentration. On the contrary, the second case is the development of suspend sediment transport at the upstream end of a channel with an initially clear flow. The third case simulates the turbidity currents in a flume with appointed flow conditions basing on a physical modelling of the LCH (Laboratory of Hydraulic Constructions) team of EPFL (Ecole Polytechnique Federale de Lausanne). Sensitivity analysis is performed for each case in order to optimize the numerical simulation, including horizontal and vertical mesh, physical (in particular the turbulence model) and numerical parameters. Calculations using TELEMAC-3D allow to reproduce the three-dimensional patterns of sediment transport correctly in general. Numerical results of each case are in agreement with the corresponding theoretical and practical considerations, demonstrating the powerful ability of TELEMAC-3D as a reliable tool to model sediment transport. Further research and practical applications can be performed using TELEMAC-3D.**

I. Introduction

Numerical morphodynamic models of increasing complexity are widely developed and used by both scientific and engineering communities over the past several decades so as to validate analytical solutions, in situ tests and furthermore predict complex applications of sediment transport. These models cover various topics in sediment transport, such as the natural or artificial bed evolution in rivers, estuaries and seas. A range of morphodynamic modeling systems like ECOMSed, Mike-21 and Delft-3D and ROMS generally include basic flow modules (from 1D to 3D), a wave propagation model and a sand transport model including suspended load and bed load. More detailed reviews can be found in other aricles like [1].

This open-source TELEMAC hydro-informatic system is adopted as our framework. Fundamental theories can be found in this key reference [2], covering the advanced topics in the application of the finite element method and the TELEMAC system as well. A thorough overview of morphodynamic modeling using the TELEMAC finite-elment system can be referred to [3], illustrating its ability to reproduce sediment transport patterns and resulting bed evolution in increasingly complex situations from small scale laboratory experiments to field scale river applications.

Considered as a raisonable tradeoff between simulation accuracy and calculation time, 2D depth-averaged modeling is thus extensively applied to medium-scale domains in the past decades. With the development of personal workstations and clusters, 3D modeling is being paid more and more attention at the moment and will turn into an inevitable trend in the future.

Concerning the sediment transport with TELEMAC system, multiple models can be utilized. Courlis, as one part of TELEMAC system, is available to model sediment transport in one dimension. For 2D modeling, the TELEMAC-2D hydrodynamic model is internally coupled to the 2D morphodynamic model SISYPHE. For 3D modeling, the suspended load is directly calculated by TELEMAC-3D, solving an additional 3D transport equation for the sediment concentration and computing the bed evolution. In most 1D or 2D models of depth-averaged sediment transport, the suspended sediment is assumed to be advected by the depth-velocity velocity. Taking into account the fact that the largest part of the sediment is transported near the bed, the depth-averaged velocity should be weighted by the verticle concentration profile. This inherent issue can be achieved by TELEMAC-3D, resulting in more precise simluations, whereas a correction factor needs to be introduced enabling results from 2D computation to approach 3D simulation result [4].

Validation tests play an important role in the development of code implementation. This paper begins by briefly describling the physical formulations used to model the sediment transport within TELEMAC-3D. It then presents three examples of validation studies that have been carried out using TELEMAC-3D. Unfortunately, the details of simulations may not be fully explained due to the space limitations.

II. Description of model formulations

A. Hydrodynamics

In this work the non-hydrostatic version is chosen and TELEMAC-3D solves the three-dimensional mass and momentum conservation equations [5]:

$$\frac{\partial u}{\partial x}+\frac{\partial v}{\partial y}+\frac{\partial w}{\partial z}=0$$
$$\frac{\partial u}{\partial t}+u\frac{\partial u}{\partial x}+v\frac{\partial u}{\partial y}+w\frac{\partial u}{\partial z}=-\frac{1}{\rho}\frac{\partial p}{\partial x}+\nu\Delta(u)+F_x$$
$$\frac{\partial v}{\partial t}+u\frac{\partial v}{\partial x}+v\frac{\partial v}{\partial y}+w\frac{\partial v}{\partial z}=-\frac{1}{\rho}\frac{\partial p}{\partial y}+\nu\Delta(v)+F_y \quad (1)$$
$$\frac{\partial w}{\partial t}+u\frac{\partial w}{\partial x}+v\frac{\partial w}{\partial y}+w\frac{\partial w}{\partial z}=-\frac{1}{\rho}\frac{\partial p}{\partial z}+\nu\Delta(w)+F_z$$
$$p=p_{atm}+\rho g(Z_s-z)+\rho_0 g\int_z^{Z_s}\frac{\Delta\rho}{\rho_0}dz+p_d$$

where u, v and w are the three-dimensional components of velocity; F_x, F_y are source terms and ν is the effective viscosity that needs to be computed by a turbulence model. The pressure is calculated in the last equation, where ρ_0 and $\Delta\rho$ are the reference density and the variation of density respectively and Z_s is the free surface elevation.

B. Sediment transport

1) Advection-dispersion equation for sediments: Here is the Cartesian coordinate form for the advection-dispersion equation in terms of seidments:

$$\frac{\partial c}{\partial t}+\frac{\partial uc}{\partial x}+\frac{\partial vc}{\partial y}+\frac{\partial wc}{\partial z}-\frac{\partial w_s c}{\partial z}=\frac{\partial \nu_t\frac{c}{x}}{\partial x}+\frac{\partial \nu_t\frac{c}{y}}{\partial y}+\frac{\partial \nu_t\frac{c}{z}}{\partial z} \quad (2)$$

where c denotes the sediment concentration; w_s is the sediment settling velocity and ν_t is the turbulent diffusivity coefficient.

2) Additional processes:

a) Hindered settling: Subroutine WCHIND models hindered concentration dependent settling velocity in TELEMAC-3D according to

$$W_C^{'}=W_C\times(1-\frac{C}{CGEL})^5 \quad (3)$$

Here, $W_C^{'}$ is hindered concentration dependent settling velocity; W_C is sediment settling velocity; C is relative sediment concentration and CGEL is sediment concentration at which sediment forms a weak soil.

b) Flocculation: In TELEMAC-3D, two formulas are provided for taking flocculation into account.

On one hand, subtoutine WCTURB models the influence of turbulence on the settling velocity basing on the article of Van Leussen [6]. The formula for flocculation is

$$W_C^{'}=W_C\times\frac{1+A\times G}{1+B\times G^2} \quad (4)$$

where $W_C^{'}$ is settling velocity depending on flocculation and W_C is settling velocity of a particular sediment class in still water; Coefficient A controls the formation of flocs by turbulence while coefficient B controls the breaking of flocs by turbulence (Both A and B are empirical values for flocculation and breakup); the dissipation parameter $G=(\epsilon/\nu)^{1/2}$ is used to represent the turbulence intensity and can be computed with a $k-\epsilon$ model.

On the other hand, subroutine SOULSBYFLOC3D computes the fall velocity of mud flocs based on the Soulsby's formulation derived from Manning's floc database [7]. The description of the formula is rather long and thus is left out here. Complete expression of Soulsby's formula can be found in the aforementioned paper.

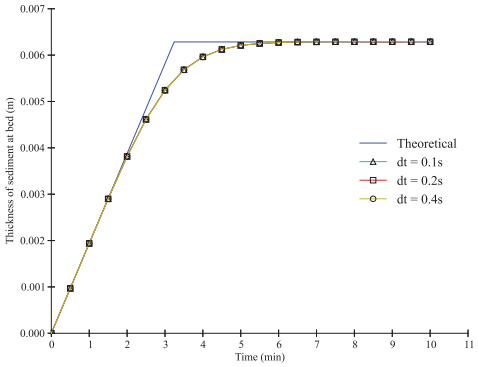

Fig. 1: Test of non-cohesive sediment

III. Validation tests

A. Settling basin

In the first case, we simulate a perfectly still settling basin containing water with an initial uniform sediment concentration. Theoretically, it takes a constant time period for a particle to fall from the water free surface to the bed, which equals the water depth divided by the sediment settling velocity.

a) Non-cohesive sediment: We assume that the initial sediment concentration is $2\,\mathrm{kg\,m^{-3}}$. The constant water depth is $5\,\mathrm{m}$ and the settling velocity of non-cohesive sediment equals $0.257\,\mathrm{m\,s^{-1}}$, hence all the sediment should fall to the bottom in $3.24\,\mathrm{min}$. Fig. 1 shows identical simulation results with different time steps.

b) Cohesive sediment: Formulae implemented in TELEMAC-3D for hindered settling and flocculation are tested as explained in section II-B2. And results are consistent with the theoretical solutions like those of non-cohesive sediment.

In order to verify that subroutine WCHIND is working well, 800 is assigned to CGEL and 40 is assigned to C (We assume that the initial sediment concentration is $50\,\mathrm{g\,L^{-1}}$ and threshold concentration for hindered velocity is $10\,\mathrm{g\,L^{-1}}$). Then result is compared between computer calculation and theoretical curve in fig. 2. The effect of hindered settling is well demonstrated.

While using Van Leussenformula, G is extremely small in this case. For this reason, variations of empirical coefficients A and B impact barely the final result. The curve is almost the same as that without taking flocculation into consideration in fig. 3.

At the last step of Soulsby formula, the mass-averaged settling velocity is calculated and compared with $0.2\,\mathrm{mm\,s^{-1}}$ and then the bigger one between them will be chosen. In this case, the shear velocity is very small and results in a very small mass-averaged settling velocity. Therefore, the final settling velocity is always $0.2\,\mathrm{mm\,s^{-1}}$. Fig. 4 proves our thought.

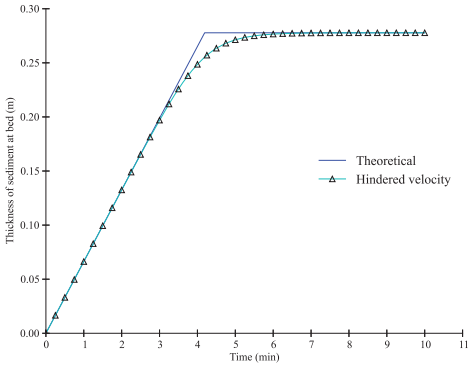

Fig. 2: Test of hindered velocity for cohesive sediment

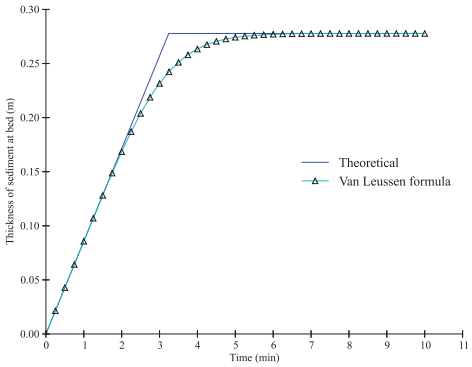

Fig. 3: Test of Van Leussen formula

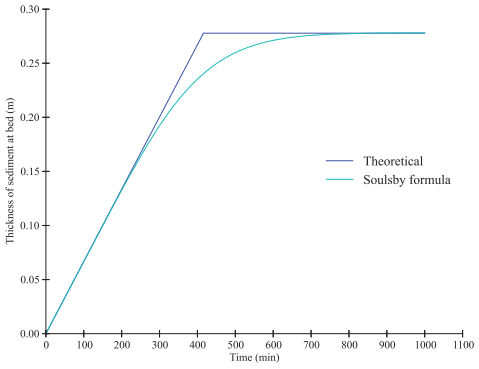

Fig. 4: Test of Soulsby formula

Further validations with respect to these two methods can be accomplished in the future cases, where the shear velocity plays a much more significant role.

c) Mixed sediment: In this situation, both non-cohesive and cohesive sediments exist simultaneously. The initial concentrations of non-cohesive and cohesive sediment are $2\,\mathrm{g\,L^{-1}}$ and $5\,\mathrm{g\,L^{-1}}$ respectively. The settling velocity of sand used in this test is $0.257\,\mathrm{m\,s^{-1}}$ while the settling velocity of mud is $0.0257\,\mathrm{m\,s^{-1}}$. There are three phases in total during the whole

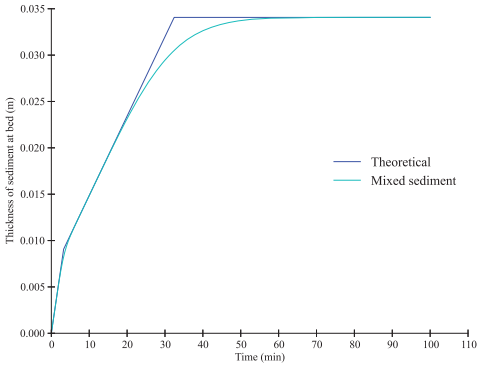

Fig. 5: Test of mixed sediment

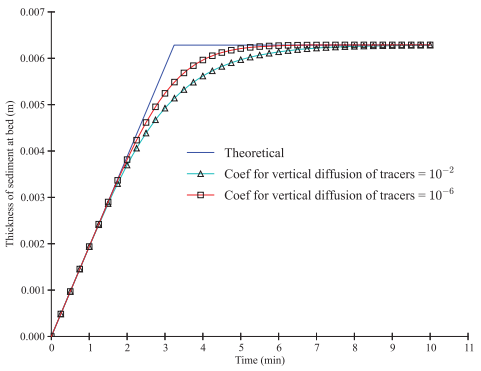

Fig. 6: Sensitivity tests of coefficient for vertical diffusion of tracers

process. In the first phase, both non-cohesive and cohesive sediments settle down simultaneously. In the second stage, all the non-cohesive sediment has already settled down and thus only cohesive sediment falls down to the bottom. In the last one, there is little sediment in the basin and almost all the sediment has reached the bottom of basin. Therefore, the bottom thickness remains nearly invariable.

Sensitivity tests show that the computed model result is sensitive to 'coefficient for vertical diffusion of tracers'. A better accordance between calculations and theorical results can be obtained with a smaller coefficient for vertical diffusion of tracers. On the contrary, time step (see fig. 1) and turbulence model won't have an impact on the simulation result. In all tests, mass balance is verified and the total quantity of sediment available in the flow does accumulate at the bed; continuity of sediment is preserved.

B. Suspended sediment transport development

This test case simulates the development of suspended sediment transport at the upstream end of a channel with an initially clear flow. Due to erosion of sediment from the bed, the suspended sediment transport rate increases with distance down the channel until equilibrium conditions are achieved even though the flow pattern is stationary. We as-

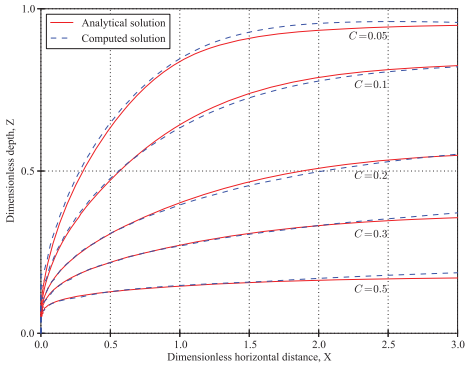

Fig. 7: Contours of equal sediment concentration along the longitudinal direction, ($A = 0.05, \lambda = 0.5$)

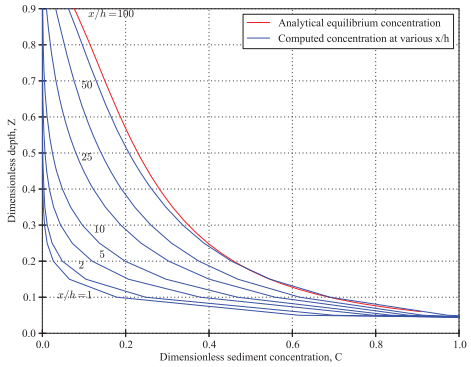

Fig. 8: Suspended sediment concentration profiles at various distances along a flume, ($A = 0.05, \lambda = 0.5$)

sume that there is no morphological change happening here and the longitudinal diffusion along the flume is neglected. In this condition, an analytical expression for the sediment concentration profiles was derived by Hjelmfelt and Lenau as a function of the distance down the channel [8]. Simulation results using TELEMAC-3D are compared with the theoretical analysis given by Hjelmfelt and Lenau. This test case has been used to validate Delft3D [9] previously. Some parameters here have been chosen identical as those in the validation case of Delft3D. The simulated flume is $120\,\mathrm{m}$ long and $10\,\mathrm{m}$ wide.

All variables of the following plots are nondimensionalized and these dimensionless variables are defined as follows:

$$\lambda = \frac{w_s}{\beta\kappa u_*},\ X = \frac{\beta\kappa u_* x}{\bar{U}h},$$
$$Z = \frac{z}{h},\ C = \frac{c}{c_a} \text{ and } A = \frac{a}{h}$$

where w_s is sediment settling velocity; β is the ratio of sediment diffusion to fluid diffusion; κ is Von Karman coefficient; u_* is the bed shear velocity; x is the longitudinal Cartesian coordinate; z is the vertical Cartesian coordinate; $\bar{U}$ is the depth-averaged GLM velocity components; h is the water depth; c is the mass sediment concentration; c_a is the mass sediment concentration at reference height and a is the height for suspended sediment concentration.

Fig. 7 shows that simulation results of TELEMAC-3D reproduce the analytical solution quite well, manifesting the adapatation of the suspended sediment concentration from an initially clear flow. Small differences for each contour do exist, but are considered to be negligeable, which is less than 5% as equilibrium conditions are approached toward the downstream end of the flume. Further investigation can be performed to reason the cause of this error, which is possibly caused by the computation scheme used in TELEMAC-3D. But parameters chosen at the moment render this test rather stable in a wide range of flow conditions and therefore it is considered to be an acceptable compromise..

Fig. 8 illustrates the gradual development of sediment concentration profile along the longitudinal direction of the flume, showing the progressive development of an equilibrium sediment concentration profile. It can be observed that the concentration profile develops step-by-step, and that equilibrium conditions have not been completely achieved even by a distance of $x/h = 100$. But we can assume reasonably that after passing through a longer distance, the sediment distribution can reach equilibrium condition. To prove this idea, another simulation is tested, where the length of the flume is changed to $1200\,\mathrm{m}$. Fig. 9 demonstrates suspended sediment concentration profile in the outlet of the 1200-m-long flume, which is in good accordance with the analytical solution Rouse profile.

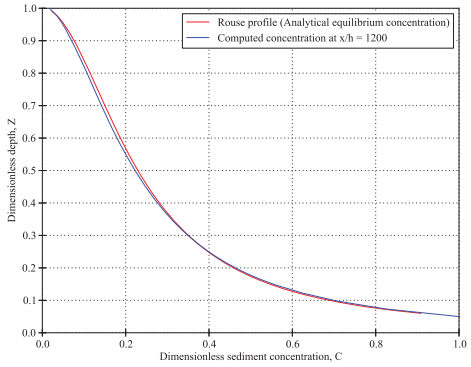

Fig. 9: Equilibrium sediment concentration profile computed $1200\,\mathrm{m}$ down a longer flume

As another check, it is quite useful to average C over the channel depth, i.e., to compute $C_{av} = \frac{1}{1-A}\int_A^1 C dZ$. C_{av} represents the average normalized concentration. The analytical solution with respect to C_{av} has been briefly given in [8] as well. Fig. 10 shows the longitudinal profile of the depth averaged suspended sediment concentration. Here the computed result is almost exactly same as the analytical solution of Hjelmfelt and Lenau.

Certain sensitivity tests were organized to observe whether some parameters have impacts on the final results. It should be pointed out that the reference height A is a crucial parameter from the standpoint of validation. The first plane above the bottom should be exclusively regarded as the reference plane, no matter the verticle mesh is equally distributed or not. Here

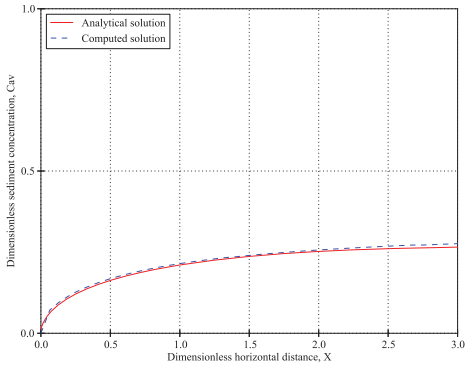

Fig. 10: Development of the depth-averaged suspended sediment concentration along a flume ($A = 0.05, \lambda = 0.5$)

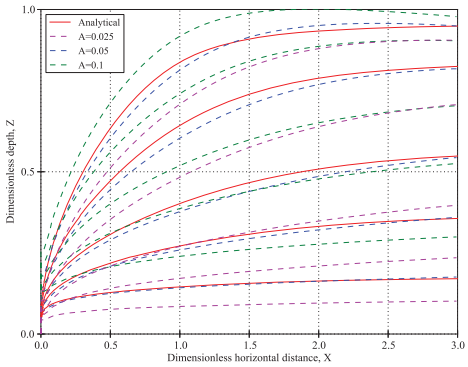

Fig. 11: Sensitivity analysis to reference height A

we anticipate 21 planes regularly spaced on the vertical. From Fig. 11, we can observe the sensible disparities among the dashed line when $A = 0.025$ or $A = 0.1$. The corresponding curves move upward if we augment the value of A. The reason lies in the relatively lower sediment concentration at higher elevations. We can approch the analytical solution while taking the first plane above the bottom as our reference plane, i.e. $A = 0.05$ here.

Several horizontal mesh resolutions were also examined. Considering that the flume width is $10\,\mathrm{m}$, mesh sizes of $1\,\mathrm{m}$, $2\,\mathrm{m}$ and $5\,\mathrm{m}$ were tested. It was proven that $2\,\mathrm{m}$ is the largest mesh size for the proper simulation of this case.

C. Turbidity currents

Turbidity currents are particle-laden gravity-driven underflows in which the particles are largely or wholly suspended by fluid turbulence [10]. The turbulence is typically generated by the forward motion of the current along the lower boundary of the domain, the motion being in turn driven by the action of gravity on the density difference between the particle-fluid mixture and the ambient fluid.

The objective of this case is to compare simulation results in TELEMAC-3D with experimental data obtained by Sabine

TABLE I: Dimensions of simulated device

Parameter	Dimension (m)
L	6.7
I	0.272
H	0.8
h	0.045
a	0.09
b	0.12

Chamoun during her PhD at LCH (EPFL). LCH team kindly made the data available for LNHE.

Experimental tests are carried out in an $8.55\,\mathrm{m}$ long, $0.272\,\mathrm{m}$ wide, and $1\,\mathrm{m}$ depth flume that can be tilted with a slope ranging from 0 to 5%. This flume is divided into three parts: the upstream part, also called the head tank ($0.8\,\mathrm{m} \times 0.272\,\mathrm{m} \times 1\,\mathrm{m}$), the main flume ($6.7\,\mathrm{m} \times 0.272\,\mathrm{m} \times 1\,\mathrm{m}$), and the downstream compartment ($1.05\,\mathrm{m} \times 0.272\,\mathrm{m} \times 1\,\mathrm{m}$). The head tank receives the water-sediment mixture from the mixing tank and is linked to the main flume by a sliding gate that, once opened, leads to the formation of the turbidity current inside the flume simulating a reservoir. Precise geometric dimensions are listed in tab. I, including sizes of inlet, outlet and the main flume. A sketch as fig. 12 is reproduced here as well so as to simplify the matching of corresponding dimensions. The parameter I and a, representing widths of the main flume and the outlet respectively, don't show up in fig. 12.

The whole experimental procedure is described as follows [11]. At the beginning of each test, the mixing tank is filled with water and a specific mass of fine powdery material (Thermoplastic Polyurethane in the case of the present study) is added until the desired concentration is obtained. Meanwhile, the main channel where the current will develop is filled with tap water up to a level of $80\,\mathrm{cm}$. Once ready, the mixture is pumped to the head tank, and returns to the mixing tank through a recirculation pipe. This recirculation lasts for a few minutes and helps in regulating the flow rate (around 1 l/s for all tests) through an electromagnetic flowmeter, insuring a good mixing and homogeneous concentrations between the two reservoirs. Before starting the test, the water level in the head tank and the main channel should be equal in order to avoid any head losses when the gate is opened and the turbidity current released. The concentration of the mixture is continuously measured using a turbidity probe placed in the head tank. Once the concentration measured reaches the desired value, the sliding gate separating the head tank from the main flume is opened and the turbidity current is released into the flume. Right at the entry of the flume, the current passes through a tranquilizer that reduces its initial turbulence scale and gives a nearly uniform horizontal distribution for the velocity field of the current. A clear water discharge is ejected through the diffusor placed right above the tranquilizer. The turbidity current then flows along the channel through a distance of 6.70 m and is monitored for the whole duration of the test. Once it reaches a location corresponding to the tested timing, the bottom outlet is opened with a specific discharge, controlled by the aforementioned valve and electromagnetic flowmeter placed downstream. The vented current reaches a basin where continuous concentration measurements

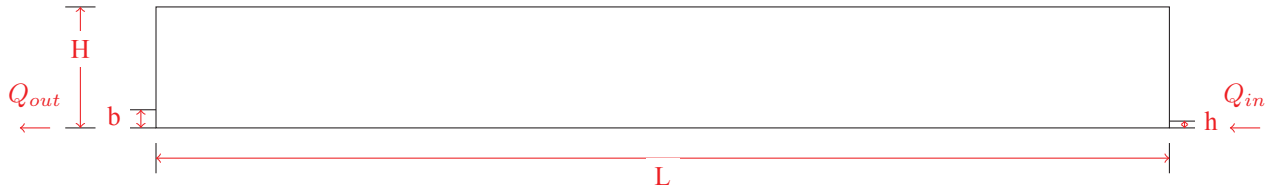

Fig. 12: Front view of the main flume

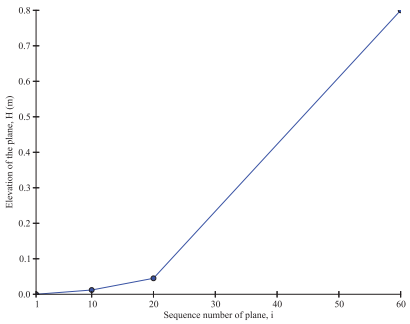

Fig. 13: Distribution of vertical cell sizes for turbidity current modelling.

TABLE II: Error analysis

Time (s)	PBIAS(%)	RMSE	RSR
51.39	17.902	0.000273	0.265
64.60	19.121	0.000365	0.265
78.00	16.895	0.000423	0.257
102.50	14.180	0.000596	0.297
133.26	10.374	0.000966	0.404
148.00	11.272	0.00114	0.438
160.89	8.573	0.00134	0.509

are achieved using a turbidity probe. Based on this, venting efficiencies are calculated for different scenarios.

Sensitivity tests indicate that the number of vertical levels should be sufficient enough to guarantee the proper simulation of turbidity currents. Thus the horizontal mesh size is equalling to $0.01\,\mathrm{m}$ and 60 irregularly spaced layers are in the vertical direction (Figure 13).

In fact, this case is very sensitive to the variation of sediment settling velocity. Besides Stokes' law, there are a number of formulae for the settling velocity of sediment particles. Benoît Camenen proposed a simple and general formula for the settling velocity of particles [12] in 2007 and a brief review can be found as well in the introduction part of this forementioned paper. Stokes' law gives a theoretical settling velocity of $1.5\,\mathrm{mm\,s^{-1}}$. According to Camenen's formula, we can obtain a settling velocity of $1.558\,\mathrm{mm\,s^{-1}}$. Here we have tested two other settling velocities, being equal to $1.3\,\mathrm{mm\,s^{-1}}$ and $1.7\,\mathrm{mm\,s^{-1}}$ respectively. Fig. 14 indicates that the computed result is quite sensitive to the settling velocity, proving that settling velocity is a crucial physical parameter in this numerical model. With a greater settling velocity, more sediment will settle down in a closer place to the inlet and less sediment can cover a rather long distance in the flume. This phenomena corresponds with our common sense. We can note that differences in the simulation results exist but seem not very obvious whether Stokes' law or Camenen's formula is chosen.

Different methods used for evaluation of numreical models have been proposed, they are represented by a number of evaluation indicators. Among these indicators, RMSE, RSR and PBIAS are calculated for the sake of assessment in this case. Here we only consider the settling velocity given by Stokes' law. Table II indicates that values of RMSE and RSR increase with respect to the time while values of PBIAS decrease with time. It can be considered that good agreement is achieved between measurements and simulations. Values of PBIAS at different moments are no more than 20. Generally speaking, values of RSR are smaller than 0.5. Judging from criterias in [13], both criterias of model evaluation are met, demonstrating a very good performance of our numerical modelling.

Although the simulation results fit the experimental data well, modifications could be made in order to improve the accuracy of the numerical models. In the earlier discussions, constant settling velocities are taken into account. But in the reality, sediment particles will not have this velocity from the very beginning. They should go through a process of flocculation. In order to solve this deficiency, the model could be improve with the use of settling velocity measurements.

Fig. 15 demonstrates features of turbidity currents during midel simulations. Beneath, screeenshots (See Figure 16) are taken from the recorded video so as to compare them qualitatively with the simulation results.

IV. Conclusion-Future work

TELEMAC-3D has already been validated across a great number of processes and their interactions. The 'tip of the iceberg' can be easily accessed in the directory of TELEMAC-3D examples. The validation tests shown in this paper have demonstrated the ability of TELEMAC-3D to model the following processes: (1) sediment settling, (2) suspended sediment transport and (3) turbidity currents. On the basis of this paper, further research will focus on the definition of benchmarks, the combinations and interactions of processes as well as more applications in the prototype-scale and real-life situations.

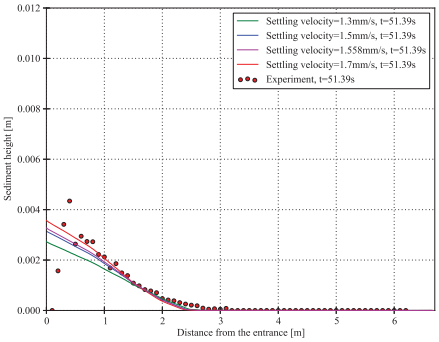

(a) t = 51.39 s

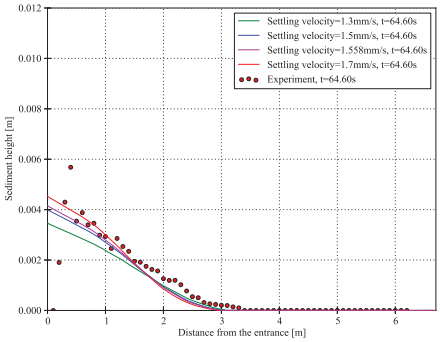

(b) t = 64.60 s

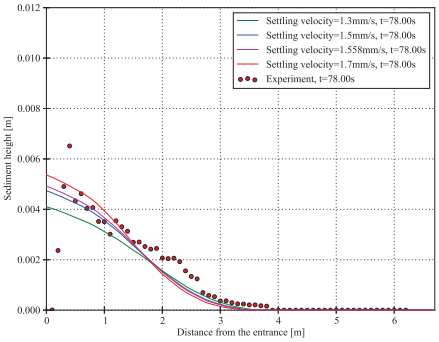

(c) t = 78.00 s

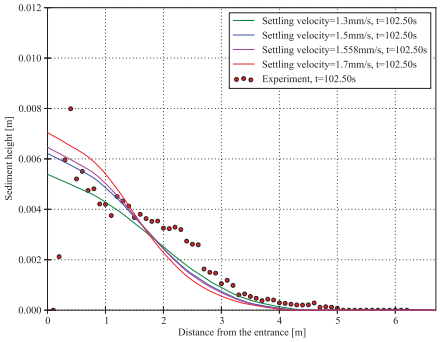

(d) t = 102.50 s

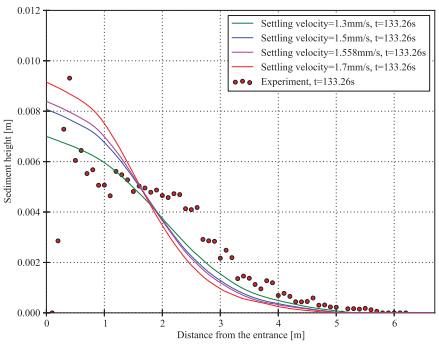

(e) t = 133.26 s

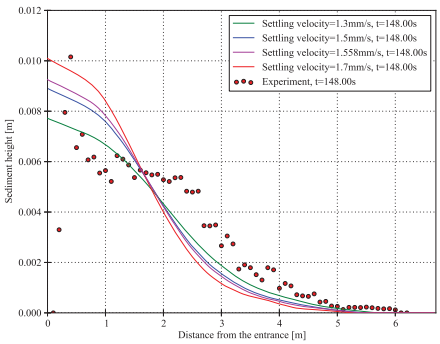

(f) t = 148.00 s

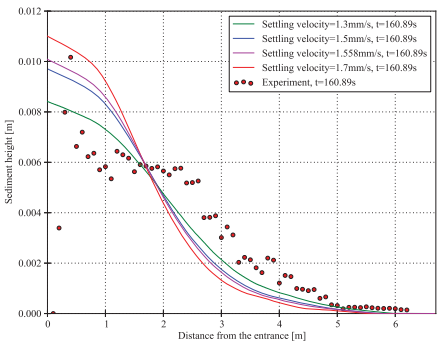

(g) t = 160.89 s

Fig. 14: Sensitivity analysis of settling velocity

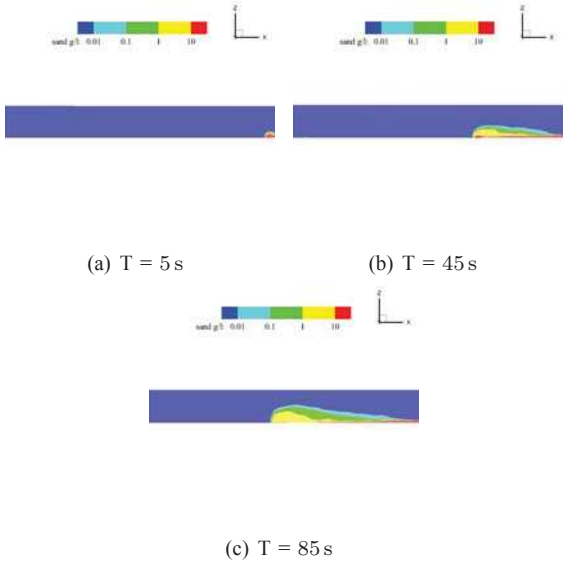

(a) T = 5 s (b) T = 45 s

(c) T = 85 s

Fig. 15: Different stages of simulated avancing turbidity currents, front view (2D)

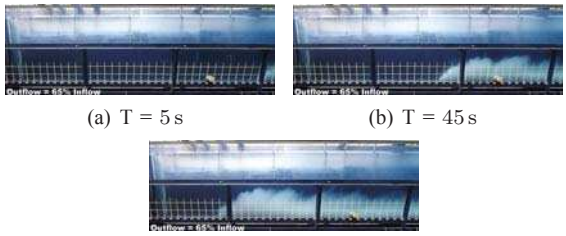

(a) T = 5 s (b) T = 45 s

(c) T = 85 s

Fig. 16: Different stages of experimental avancing turbidity currents, front view (2D)

Acknowledgment

The authors would like to thank Sabine Chamoun for providing the experimental data of the third test. Gratitudes are as well extended towards Giles Lesser for his kind help in the second validation case.

References

[1] Athanasios (Thanos) N Papanicolaou, Mohamed Elhakeem, George Krallis, Shwet Prakash, and John Edinger. Sediment transport modeling review—current and future developments. *Journal of Hydraulic Engineering*, 134(1):1–14, 2008.

[2] Jean-Michel Hervouet. *Hydrodynamics of free surface flows: modelling with the finite element method*. John Wiley & Sons, 2007.

[3] Catherine Villaret, Jean-Michel Hervouet, Rebekka Kopmann, Uwe Merkel, and Alan G Davies. Morphodynamic modeling using the telemac finite-element system. *Computers & Geosciences*, 53:105–113, 2013.

[4] N Huybrechts, C Villaret, and JM Hervouet. Comparison between 2d and 3d modelling of sediment transport: application to the dune evolution. In *River Flow*, 2010.

[5] OPERATING MANUAL. Telemac modelling system. 2016.

[6] W. van Leussen. *Estuarine macroflocs and their role in fine-grained sediment transport: Macrovlokken en hun bijdrage aan de slibtransporten in Estuaria*. Universiteit Utrecht, Faculteit Aardwetenschappen, 1994.

[7] RL Soulsby, AJ Manning, J Spearman, and RJS Whitehouse. Settling velocity and mass settling flux of flocculated estuarine sediments. *Marine Geology*, 339:1–12, 2013.

[8] A t Hjelmfelt and Charles Walter Lenau. Nonequilibrium transport of suspended sediment. In *Journal of the Hydraulics Division: Proceedings of the American Society of Civil Engineers*, number HY7, 1970.

[9] GR Lesser, JA Roelvink, JATM Van Kester, and GS Stelling. Development and validation of a three-dimensional morphological model. *Coastal engineering*, 51(8):883–915, 2004.

[10] Eckart Meiburg and Ben Kneller. Turbidity currents and their deposits. *Annual Review of Fluid Mechanics*, 42:135–156, 2010.

[11] Sabine Chamoun. Experimental set-up. Technical report. Personal communication.

[12] Benoît Camenen. Simple and general formula for the settling velocity of particles. *Journal of Hydraulic Engineering*, 133(2):229–233, 2007.

[13] Daniel N Moriasi, Jeffrey G Arnold, Michael W Van Liew, Ronald L Bingner, R Daren Harmel, and Tamie L Veith. Model evaluation guidelines for systematic quantification of accuracy in watershed simulations. *Transactions of the ASABE*, 50(3):885–900, 2007.